Power Leakage, Characteristic Impedance, and Leakage-Transition Behavior of Finite-Length Stub Sections of Leaky Printed Transmission Lines

Nirod K. Das, *Member, IEEE*

Abstract— **Power leakage and leakage transition phenomena in finite-length stub sections are studied for slot- as well as strip-type leaky transmission lines. A three-dimensional (3-D) method of moments is used for the rigorous analysis of the stub sections. The results reveal several important characteristics of power leakage in printed circuits that are not obtainable from the two-dimensional (2-D) analyses of ideal infinite-length lines. A new definition of the characteristic impedance for a leaky printed transmission line is proposed, which is shown to correctly model the impedance behavior of the finite-length sections. It is noted that the standard definitions of characteristic impedance, commonly used for nonleaky transmission lines, may not apply to practical circuits when leakage exists. Further, the leakage transition behavior in the finite-length sections, operated around a "mode-transition" region, is explained from the 3-D analysis results. Leakage analyses of ideal infinite-length lines can not model such transition excitation in finite-length circuits.**

I. Introduction

It has been recognized that under certain conditions of frequency and/or physical parameters, the dominant mode of a multilayered printed transmission line can leak power transversally due to coupling to the surface-wave mode(s) [1]–[5]. Such leakage effects demand careful attention in multilayer integrated circuits, and multilayer feed networks for integrated phased arrays [6], which could otherwise result in catastrophic coupling between adjacent circuit components. Coupling between two transmission lines placed electrically far apart, established through such leakage power, can also be used to one's advantage for designing novel printed circuit couplers. New analyses to model the leakage in printed transmission lines have been presented using a rigorous spectral domain method [2] that has been successfully applied to a variety of geometries in [2]–[4] and [7] as well as using a mode-matching approach [1]. However, all the above analyses assume an ideal infinite-length line. In order to understand the possible leakage phenomena in practical printed circuits, it is important to investigate the leakage in realistic finite-length sections. Several important characteristics of power leakage in practical circuits can not be explained using the analyses that ideally assume an infinite-length transmission line.

Manuscript received December 21, 1994; revised December 18, 1995. This work was supported in part by the US Army Research Office, Research Triangle Park, NC

The author is with Weber Research Institute, Department of Electrical Engineering, Polytechnic University, Farmingdale, NY 11735 USA.

Publisher Item Identifier S 0018-9480(96)02332-0.

None of the research to date on power leakage has investigated the impedance characteristics of leaky printed transmission lines. It is essential to define an "equivalent characteristic impedance," that can correctly model the impedance behavior of finite-length sections under leakage conditions. However, due to the "nonconventional" nature of a leaky printed transmission line [2], fundamental difficulties arise. The standard definitions of characteristic impedance, commonly used for conventional nonleaky transmission lines, may not be applicable when leakage exists.

Complex mode characteristics of an ideal infinite-length leaky line in the vicinity of a "mode-transition" region have been studied [5]. However, it is of interest to understand the leakage transition behavior on a practical finite-length structure operated in this region. Unfortunately, such leakage behavior on finite-length circuits can not be properly explained from the mode characteristics of an ideal infinite-length line. The actual excitation on a finite-length section would be a complex combination of the multiple modes of the infinite-length line, with other discontinuity effects. Rigorous 3-D analysis of the finite-length circuit with a realistic feeding source may have to be performed in order model such excitation behavior.

Further, it has been shown in [2] that the fields of a leaky printed transmission line ideally of infinite length grows exponentially in transverse directions to infinity at large distances. As explained in [2], this "nonconventional" infinite growth is a physically valid behavior for the ideal situation of an infinite-length leaky line. This does not violate the radiation condition of the electromagnetic theory due to the associated infinite input power (because $e^{-\alpha x}$ grows to ∞ as $x \rightarrow -\infty$) of the infinite-length line. Of course, for a practical situation of a finite-length leaky line, the fields can never grow indefinitely in transverse directions. As the radiation condition dictates, the fields in the finite-length case must eventually decay down to zero at sufficiently large distances. Hence, the obvious questions do arise: 1) How far in transverse directions do the fields of a finite-length leaky line grow? and 2) how does this growth compare and contrast with the exponential growth predicted from the analysis of an ideal infinite-length line? Study of finite-length sections of leaky transmission lines will be essential in order to evaluate such field-spreading behavior. In a practical circuit, this will help determine the extent of the unwanted coupling between neighboring components, established due to the power leakage.

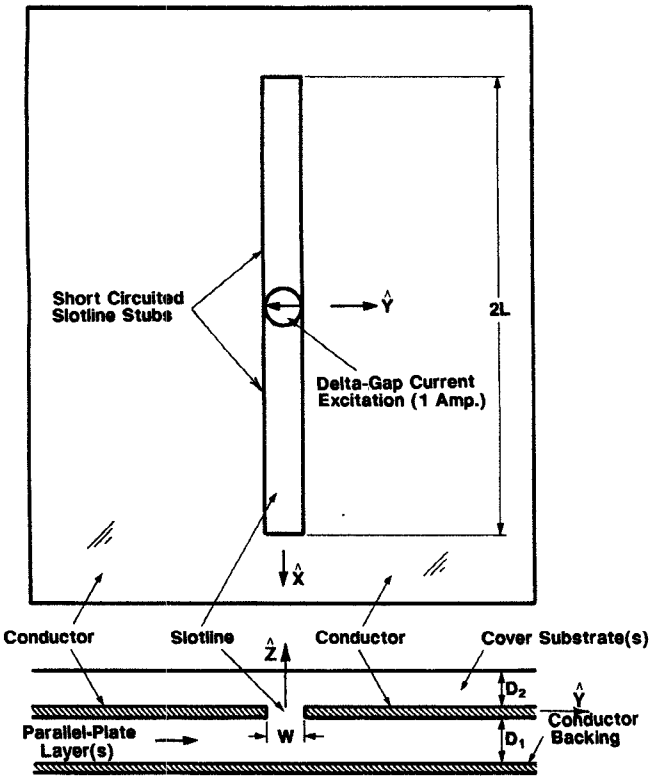

Fig. 1. Geometry of a finite-length section of an example leaky conductor-backed slotline in a general multilayer configuration, excited by a small current-source at the center.

This paper attempts to answer such questions of practical significance discussed above. A rigorous 3-D moment method analysis of finite-length leaky transmission line stubs, excited by a delta-gap source along the line, is used for this investigation. The analysis is applied to strip- as well as slot-type leaky lines, demonstrating the leakage concepts in different situations. Section II describes the 3-D moment method analysis. The results of the 3-D analysis for radiation as well as surface-wave leakage in selected finite-length stub sections are compared and contrasted with the results from an ideal infinite-length analysis. Section III presents the new definition of the characteristic impedance for leaky lines, and its validity is demonstrated via comparison with the rigorous analysis. Finally, Section IV presents the results for the leakage transition effects. In all our discussions, the scope of a "transmission line," or a "line," is limited to printed geometries only.

II. Analysis of Finite-Length Stub Sections of Leaky Transmission Lines

Fig. 1 shows a finite-length stub section of a leaky conductor-backed slotline, used here as an example geometry for the analysis. The finite-length section of length $2L$ is excited at the center by a parallel delta-gap current source of unit amplitude, and may be configured within a general multilayer environment. Such a conductor-backed slotline can exhibit leakage to the parallel-plate mode below the slot, and is used here as a representative leaky transmission line. The analysis can be applied, as discussed, to other strip- as well as slot-type leaky transmission lines, with single or multiple sources at arbitrary locations along the line.

We analyze the finite-length section of Fig. 1 using a 3-D moment method analysis in the spectral domain. Similar moment method analyses have been commonly used for printed circuit problems [8]–[12] that can be referred to for detailed background. We close the slot, and equivalently replace the unknown electric fields, $\bar{E}_s(x, y)$, across the slotline by magnetic current distributions, $\pm\bar{M}_s(x, y)$. The two magnetic current distributions, $+\bar{M}_s$ and $-\bar{M}_s$, of equal magnitude but oppositely directed to each other, are placed above and below the ground plane, respectively

$$\pm\bar{M}_s(x, y) = \pm\bar{E}_s(x, y) \times \hat{z}. \tag{1}$$

Now, the unknown $\bar{M}_s(x, y)$ is solved by expanding it by a set of $(2N + 1)$ piecewise sinusoid (PWS) basis functions with unknown coefficients, V_i [9], [12]

$$\bar{M}_s(x, y) = \sum_{i=-N}^{N} V_i \bar{f}_i(x) h(y), \tag{2}$$

$$h(y) = \frac{1}{\pi\sqrt{(W/2)^2 - y^2}}, \tag{3}$$

$$\bar{f}_i(x) = \hat{x}\frac{\sin\left[k_e'(L_i - |x_i|)\right]}{\sin\left(k_e' L_i\right)}; \quad |x_i| \le L_i,$$
$$= 0; \quad \text{elsewhere}, \tag{4}$$

$$L_i = \frac{L}{N+1}, \tag{5}$$

$$x_i = x - iL_i = x - \frac{iL}{N+1}. \tag{6}$$

It is assumed that $\bar{M}_s$ is x-directed, or equivalently $\bar{E}_s$ is y-directed. This is known to be a good approximation for narrow slots, neglecting any small longitudinal (x-directed) slot-fields. The transverse variation, $h(y)$, across the slot includes an appropriate edge condition to accommodate for the electric field singularities at the slot edges. The k_e' in (4) is an arbitrary numerical parameter. This parameter should preferably be chosen close to the effective phase constant of the transmission line [2] in order to achieve better convergence with respect to the number of basis functions, $2N + 1$. As a general guidance to selecting N in (2), about ten or more PWS modes over one guide wavelength should be adequate for accurate results.

The $(2N + 1)$ unknown basis coefficients in (2) are solved using a Galerkin testing procedure in the spectral domain, enforcing the continuity of the magnetic field across the slot. This results in a complete set of $(2N + 1)$ linear equations to be solved for all V_i's

$$\sum_{j=-N}^{N} V_i Y_{ij} = I_i; \quad i = -N, \cdots, +N, \tag{7}$$

$$Y_{ij} = \frac{1}{4\pi^2}\int_{-\infty}^{+\infty}\int_{-\infty}^{+\infty} (\tilde{G}_{H_x 2M_x}(k_x, k_y)+\tilde{G}_{H_x 1M_x}(k_x, k_y)) \cdot F_i(k_x)F_j^*(k_x)|H(k_y)|^2\, dk_x\, dk_y, \quad (8)$$

$$I_i = \begin{cases} 1; & \text{for } i = 0, \\ 0; & \text{otherwise} \end{cases} \quad (9)$$

where $H(k_y)$ and $F_i(k_x)$ are, respectively, the Fourier transforms of the spatial distribution functions, $h(y)$ and $f_i(x)$, defined in (3), (4). $\tilde{G}_{H_x 2M_x}$ and $\tilde{G}_{H_x 1M_x}$ are, respectively, the spectral-domain multilayer Green's functions [13], [14] for the x-component of the magnetic field, produced by an x-directed magnetic source. Both the source and the field points are slightly above the ground plane for $\tilde{G}_{H_x 2M_x}$, whereas they are slightly below the ground plane for $\tilde{G}_{H_x 1M_x}$. In (7) and (9), I_i is the excitation to the ith basis function from the source current. This excitation is provided by the delta-gap current source (see Fig. 1) at the center of the slot-section that directly couples only to the zeroth ($i = 0$) basis function at the center. Excitation at other positions along the slotline is handled by setting the appropriate excitation elements, I_i.

After the unknown coefficients V_i's are solved from (7), the total slot field, $\bar{E}_s(x, y)$, can be obtained using the equations (1)–(6). Then, any cross-sectional field component at an arbitrary location around the slotline can be computed using the corresponding Green's function component and the Fourier transforms of the slotfield, $\tilde{\bar{E}}_s(k_x, k_y)$, via an inverse spectral integration.

It may be noted that the spectral-domain evaluation of the moment matrix elements in (8) does not require any special deformation of the integration contour in order to account for the leakage phenomenon. The two-dimensional (2-D) moment integrations are performed along the real spectral axes (k_x, k_y) in the same way for cases with or without any power leakage. In distinct contrast, the spectral-domain analysis of an ideal infinite-length leaky transmission line [2], [15] is performed using a one-dimensional integration on the complex k_y plane. This requires a special contour deformation procedure off the real spectral (k_y) axis, around specific complex pole(s).

Extension of this analysis to strip-type lines is possible by replacing the equivalent magnetic currents on the slot plane of Fig. 1 by the electric currents on the strips of a strip-type line. In addition, the parallel delta-gap current source of excitation in Fig. 1 should be replaced by a series delta-gap voltage source for a strip-type line. The effect of the electric current source and any arbitrary substrate layers can be accommodated via use of the proper Green's functions [13], [14]. The zero tangential electric field on the strip surface is the required boundary condition in a stripline case, instead of the continuity of the electric field enforced across the slot in (8).

A. Results

Fig. 2 shows the computed slot-voltage for a conductor-backed slotline section of Fig. 1, compared with the similar results for a nonleaky air-slotline. Clearly, the conductor-backed slotline exhibits an attenuating behavior, in contrast to the nondecaying standing-wave behavior for the air-slotline. This result supports that finite sections of certain transmission lines can exhibit significant attenuation, even when material losses are absent, due to coupling to the characteristic surface mode(s). This is consistent with the recent prediction from an ideal infinite-length analysis [2].

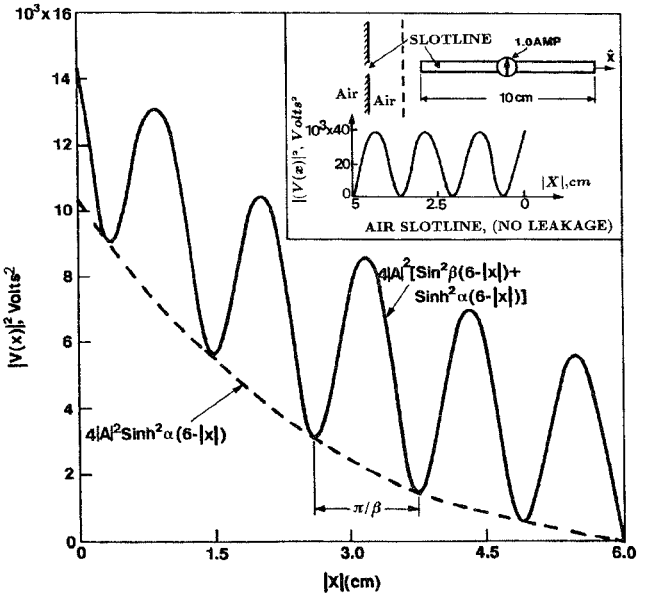

Fig. 2. Voltage across the slot, computed from a full-wave finite-length analysis of the geometry of Fig. 1. W = 0 3 cm, no cover substrate, uniform dielectric between parallel plates (ϵ_r = 2 55, thickness = 0.801 cm), L = 6 cm, frequency = 10 GHz. Inset is the slot-voltage, computed from the same full-wave finite-length analysis, across an air-slotline section ($2L$ = 10.0 cm), fed at the center by a delta-gap 1.0 A current-source. Slot width = 0.1 cm, frequency = 10 GHz. Notice, the former geometry is clearly leaky, whereas the latter is nonleaky.

For the leaky conductor-backed slotline in Fig. 1, we assume an $e^{\mp j\beta x}e^{\mp \alpha x} = e^{\mp \gamma x}$ propagation, and a total reflection at the short-circuited ends with a reflection coefficient $\Gamma = -1$. With these assumptions, the slot-voltage, $V(x)$, can be written as

$$V(x) = A[e^{+\gamma(L-|x|)} - e^{-\gamma(L-|x|)}] = 2A\sinh[\gamma(L-|x|)], \quad (10)$$

$$|V(x)|^2 = 4|A|^2[\sin^2\beta(L-|x|) + \sinh^2\alpha(L-|x|)]. \quad (11)$$

In Fig. 2 the lower envelope of the $|V(x)|^2$ pattern is $4|A|^2\sinh^2\alpha(L-|x|)$. The additional oscillating function, superimposed above the lower envelope, is $4|A|^2\sin^2\beta(L-|x|)$. Therefore, A and β can be calculated from the amplitude and the periodicity, respectively, of the oscillating part. Using the above value of A, the attenuation constant, α, can then be derived from the lower envelope. The phase constant, β, and the attenuation constant, α, obtained using the above procedure are compared in Fig. 3 with the respective values from the analysis of an ideal infinite-length line [2]. Similar comparison between the results from a finite- and an infinite-length analyses of a two-layer stripline geometry are presented in Fig. 4. As has been mentioned earlier, the analyses of an infinite-length and a finite-length leaky transmission lines are

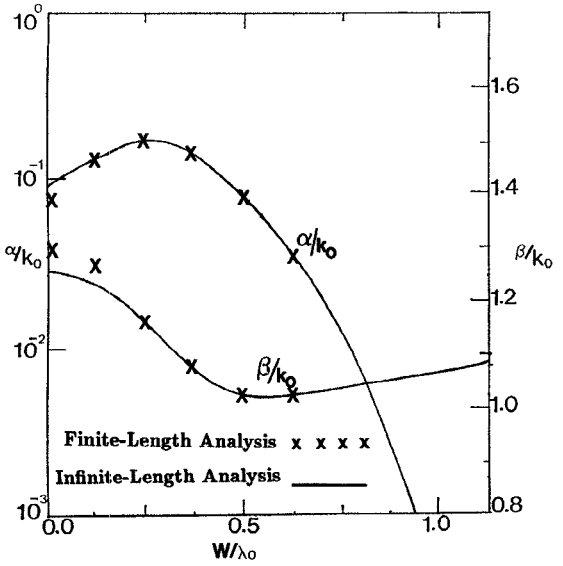

Fig. 3. The phase, β, and attenuation, α, constants of the conductor-backed slotline of Fig. 2, for different values of W, derived from the voltage distribution on a finite-length section, as compared to those obtained from an ideal infinite-length analysis.

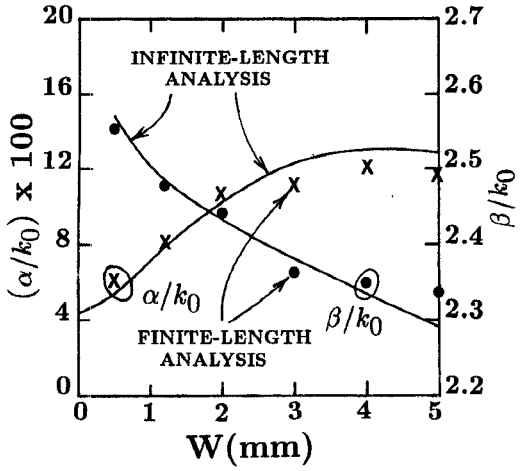

Fig. 4. The phase, β, and attenuation, α, constants of a two-layer stripline of Fig. 15 with $h = 10$ mils, derived from the current distribution on a finite-length section, as compared to those obtained from an ideal infinite-length analysis. The finite-section used for the analysis is a stub section of length, L, open circuited at both ends and excited by a series delta-gap voltage source at the center (see Fig. 16). W is the width of the stub. The poorer comparison for larger W is due to the gradual excitation of the additional nonleaky mode (shown in Fig. 15)

fundamentally different. However, it is interesting to see that the two sets of results in Figs. 3 and 4 are quite close to each other. This confirms that, in spite of the nonstandard nature of an ideal infinite-length leaky line with indefinitely growing fields, the propagation characteristics predicted assuming the infinite-length idealization is still relevant and valid for practical finite-length sections. As will be explained, however, the infinite-length idealization will fail to model the impedance, field-spreading, and leakage-transition behavior of finite-length sections.

The results of Figs. 2–4 are for example cases that leak power to a surface parallel-plate mode. Similar leakage can also occur due to radiation to a semi-infinite medium above or below a transmission line [2]. The slot-voltage of an example slotline section with two semi-infinite dielectric media on its two sides is plotted in Fig. 5. In agreement with the prediction from an infinite-length analysis of [2], this finite-length geometry also exhibits an attenuating behavior. Interestingly, the phase, β, and attenuation, α, constants derived from Fig. 5 are found to match with the results from a complex-branch plane analysis [2] (which is fundamentally different) of the infinite-length line.

The transverse field component, H_y, of the finite-length geometry of Fig. 2 is computed using the 3-D moment method analysis. The results are compared in Fig. 6 with the exponential growth derived from a 2-D analysis of an ideal infinite-length conductor-backed slotline [2]. The growing nature of the field of the finite-length case, for a limited region away from the center, is clearly seen. The growth rate in this region agrees well with the ideal exponential growth of the infinite-length line. However, beyond about 3.0 cm away from the center the field amplitude for the finite-length case has decayed down to a low level, satisfying the radiation condition of the electromagnetic theory, whereas for the ideal infinite-length line the field continues to grow indefinitely. As these results suggest, the exponential transversal growth of an ideal infinite-length leaky line should be interpreted as valid for practical situations only up to a limited distance away from the central region, but considered nonphysical sufficiently far away. In order to determine the actual field-spreading behavior of a practical finite-length section, a rigorous 3-D analysis must be performed. Information about such field-spreading is valuable for practical circuit design and understanding.

III. Characteristic Impedance of Leaky Transmission Lines

All research to date [1]–[5] on leakage from printed lines has concentrated only on the propagation characteristics. The impedance characteristics of leaky lines have not been investigated. It is important to correctly define a characteristic impedance, Z_c, for an ideal infinite-length leaky line that can be useful for a circuit modeling of practical finite-length sections. However, defining such an "equivalent characteristic impedance" is made complicated due to the nonconventional growing fields of the infinite-length leaky line. A standard power-voltage definition [Z_c = (voltage)^2/(cross-sectional power)], or a power-current definition [Z_c = (cross-sectional power)/(current)^2] of the characteristic impedance would not apply under this situation. Due to the growing nature of the transverse fields, which increase to infinity at large distances, the total cross-sectional power would become infinitely large. This will result in a zero or an infinite value of the characteristic impedance, if a power-voltage or a power-current definition is used, respectively. Of course, these trivial values are not practically meaningful for circuit modeling. The voltage-current definition (Z_c = voltage between the two conductors/the total current) would also not work. The strong non-TEM and nonconservative nature of the leakage fields can result in invalid calculation of the

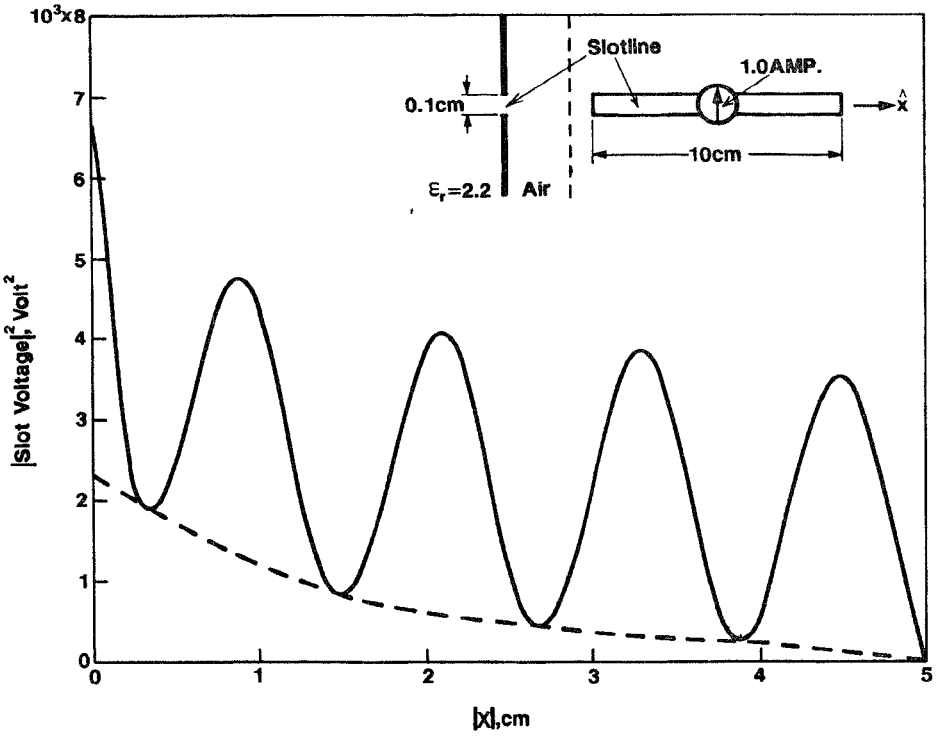

Fig. 5. Variation of the slot-voltage along a finite-length slotline section with two semi-infinite dielectric mediums on its two sides (air and $\epsilon_r = 2.2$). $W = 0.1$ cm, $2L = 10$ cm, frequency = 10 GHz. $\beta/k_0 = \sqrt{1.6}$ and $\alpha/k_0 = 0.07$, as calculated from this voltage distribution. The corresponding values obtained from an infinite-length analysis [2] are, $\beta/k_0 = \sqrt{1.5}$ and $\alpha/k_0 = 0.068$.

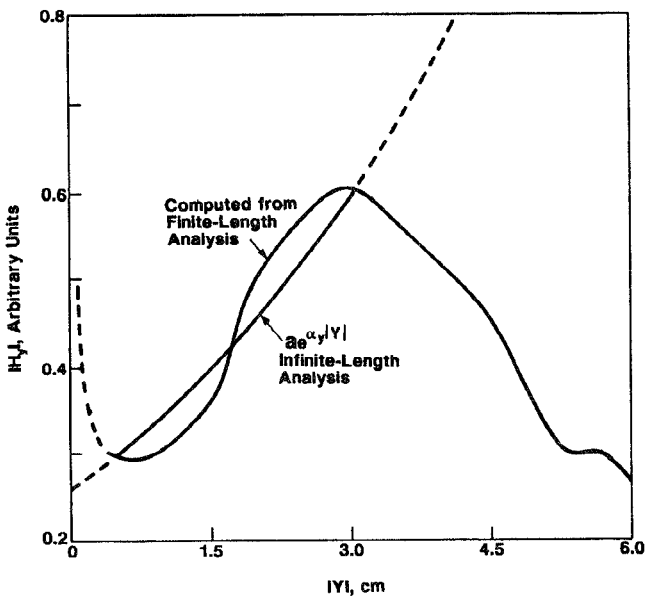

Fig. 6. Transverse variation of the y-component of the magnetic field, H_y, for the conductor-backed slotline geometry of Fig. 2, at $x = 3.0$ cm, computed from a 3-D moment method analysis of the finite-length geometry. The exponential variation predicted from an ideal infinite-length analysis is also shown for comparison.

characteristic impedance. This is due to the strong ambiguity in defining the voltage of a strip-type leaky line for a given strip current, or the total current of a slot-type leaky line for a given slot voltage.

We attempt to provide a suitable definition of the "equivalent characteristic impedance" of a leaky line that can be used for circuit modeling purposes. Shown in Fig. 7, a transverse field distribution of an infinite-length leaky line has been decomposed into two distinct parts [2]. The part that increases exponentially in transverse directions is excited due to coupling to the characteristic surface-mode of the substrate structure. This part is referred to as the "growing" field. When this growing field is extracted out of the total field distribution, the remaining part is tightly confined to the central guiding region, and is referred to as the "bound" field. The bound parts of the transverse fields actually carry the guided signal along the central region of the transmission line, and closely resemble the standard transmission line fields with a quasi-TEM-like behavior. Therefore, these bound transmission line-like fields are expected to be "seen" by a circuit element connected across the leaky line. On the other hand, the growing fields are only loosely attached to the central guiding region that are responsible for distributed radiation loss from the transmission line. These radiation fields are not a part of the quasi-TEM guided fields, and therefore, would not be "seen" across the line in a circuit sense.

We analytically extract out the growing parts from the total transverse fields of an infinite-length line, and then compute the power due to the remaining bound fields. A characteristic impedance defined using this bound-mode power, referred to as the "bound mode characteristic impedance," is shown to correctly model the input impedance behavior of finite-length stub sections. In the following we derive the bound-mode power for a conductor-backed slotline that can be similarly extended for any other leaky line. The transverse field components of an ideal infinite-length line can be expressed in

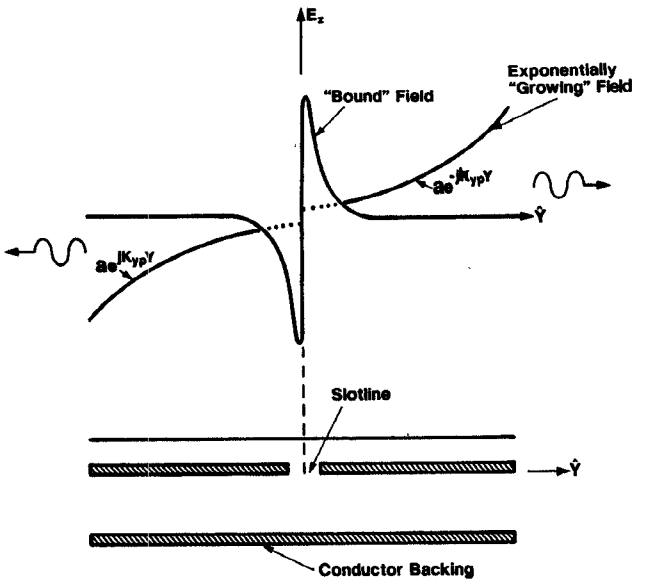

Fig. 7. Decomposition of the transverse variation of a field component, E_z, of an ideal infinite-length leaky transmission line (a conductor-backed slotline geometry, for example) into 1) the "bound" field tightly confined to the central guiding region; and 2) the exponentially "growing" field due to the excitation of a characteristic surface mode. The field is plotted along a transverse (y) line below the slot, where the parallel-plate mode exists. The growing field would not exist above the slot. Also note that the example field, E_z, is shown with an odd symmetry about the origin, but in general the field can have an odd or an even symmetry.

the spectral domain using the Fourier transform of the strip-currents or slot-fields, respectively, for a strip- or slot-type transmission line, via spectral Green's functions. For a leaky conductor-backed slotline propagating in the $\hat{x}$ direction (see Fig. 1 for cross-sectional geometry), assume the electric field, $\bar{E}_s$, distribution across the slot

$$\bar{E}_s = \hat{y} V_0 h(y) e^{-jk_e x}. \tag{12}$$

This field distribution is equivalent to two magnetic currents $+\bar{M}_s$ and $-\bar{M}_s$, respectively-placed above or below the slot, where

$$\pm\bar{M}_s(x, y) = \pm\bar{E}_s(x, y) \times \hat{z} = \pm\hat{x} V_0 h(y) e^{-jk_e x}. \tag{13}$$

With this expression for the slot-field, a cross-sectional field component, for example the z-component of electric field, $E_z(y, z)$, can be expressed as

$$\begin{aligned} E_z(y, z) &= \frac{1}{2\pi}\int_{-\infty, C}^{+\infty} \tilde{E}_z(k_y, z) e^{jk_y y}\, dk_y \\ &= \frac{V_0}{2\pi}\int_{-\infty, C}^{\infty} \tilde{G}_{E_z M_x}(k_y, z) H(k_y) e^{jk_y y}\, dk_y, \end{aligned} \tag{14}$$

$$\begin{aligned} \tilde{G}_{E_z M_x}(k_y, z) &= -\tilde{G}_{E_z 1 M_x}(-k_e, k_y, z); \quad z < 0, \\ &= +\tilde{G}_{E_z 2 M_x}(-k_e, k_y, z); \quad z > 0 \end{aligned} \tag{15}$$

where $H(k_y)$ is the Fourier transform of $h(y)$. With similar notation used in (8), and also to be used for other field components, $\tilde{G}_{E_z 2 M_x}(k_x, k_y, z)$ and $\tilde{G}_{E_z 1 M_x}(k_x, k_y, z)$ are, respectively, the spectral Green's functions [13], [14] for E_z valid above and below the ground plane ($z > 0$ or $z < 0$), respectively produced by an x-directed magnetic current source placed slightly above or below the ground plane. Notice that the k_x spectral parameter in the Green's functions have been substituted by $-k_e$ in (15) which accounts for the $e^{-jk_e x}$ variation along the transmission line.

The required contour, C, of the inverse spectral integration in (14) is deformed around the poles, $\pm k_{yp}$, on the complex k_y plane (see Fig. 8)

$$k_{yp} = \sqrt{\beta_p^2 - k_e^2}; \quad \mathrm{Im}\,(k_{yp}) > 0 \tag{16}$$

where β_p is the propagation constant of the characteristic surface-wave mode (for example, the parallel-plate mode of a conductor-backed slotline) on the (x, y) plane. It may be noted that the exponentially growing part in Fig. 7 is due to the residue contribution of the singularities at $\pm k_{yp}$ [2]. This growing field can, therefore, be extracted out by extracting these poles at $\pm k_{yp}$ from the spectral Green's functions. The remaining bound fields, for example, $E_{zb}(y, z)$, of the total field, $E_z(y, z)$, can now be written as

$$\begin{aligned} \dot{E}_{zb}(y, z) &= \frac{1}{2\pi}\int_{-\infty, realaxis}^{+\infty} \tilde{E}_{zb}(y, z) e^{jk_y y}\, dk_y \\ &= \frac{V_0}{2\pi}\int_{-\infty, realaxis}^{+\infty} [\tilde{G}_{E_z M_x}(k_y, z) H(k_y) \\ &\quad - \tilde{E}_{zg}(k_y, z)] e^{jk_y y}\, dk_y. \end{aligned} \tag{17}$$

In the above expression, $\tilde{E}_{zg}(k_y, z)$ is the transform of the exponentially growing part that can be expressed using the residue theory as

$$\begin{aligned} \tilde{E}_{zg}(k_y, z) &= \frac{\tilde{G}^R_{E_z M_x}(-k_{yp}, z) H(-k_{yp})}{k_y + k_{yp}} \\ &\quad + \frac{\tilde{G}^R_{E_z M_x}(k_{yp}, z) H(k_{yp})}{k_y - k_{yp}}. \end{aligned} \tag{18}$$

$\tilde{G}^R_{E_z M_x}(\pm k_{yp}, z)$ is the residue of $\tilde{G}_{E_z M_x}(k_y, z)$ at $\pm k_{yp}$ that can be analytically or numerically derived from the expressions of $\tilde{G}_{E_z M_x}(k_y, z)$ [14].

Now, after the bound fields are extracted from each field component, the "bound mode power," P_b, can be computed as

$$\begin{aligned} P_b = \frac{1}{2\pi}\int_{-\infty, realaxis}^{+\infty} \int_{-\infty}^{\infty} &[\tilde{E}_{yb}(k_y, z) \tilde{H}^*_{zb}(k_y, z) \\ &- \tilde{E}_{zb}(k_y, z) \tilde{H}^*_{yb}(k_y, z)]\, dz\, dk_y. \end{aligned} \tag{19}$$

The z-integration in (19) can often be done analytically using the simple z-dependence of the spectral Green's functions [13], [14]. The spectral integration of (19) with respect to k_y can be evaluated along the real k_y axis, because the integrands no longer contain the singularities at $\pm k_{yp}$. It should be noted that the standard spectral-domain expression of transverse power commonly used for nonleaky transmission lines, if applied to

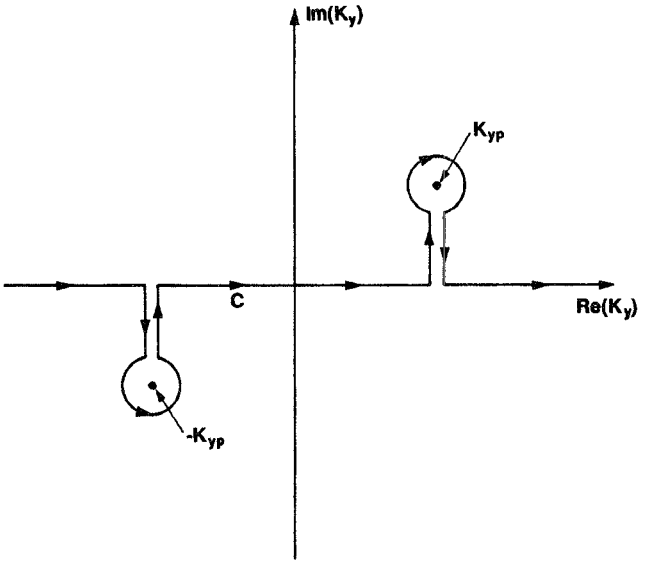

Fig. 8. Contour of integration, C, for computation of the total field component (including growing and bound fields) of a leaky transmission line. However, the bound field, after the growing field is extracted out, can be computed by a spectral inverse integration along the real axis.

a leaky line, could result in a nonphysical value, P_b', quite different from the bound mode power, P_b, given by (19)

$$P_b' = \frac{1}{2\pi}\int_{-\infty,\,real\,axis}^{+\infty}\int_{-\infty}^{+\infty}[\tilde{E}_y(k_y, z)\tilde{H}_z^*(k_y, z) - \tilde{E}_z(k_y, z)\tilde{H}_y^*(k_y, z)]\,dz\,dk_y. \quad (20)$$

In (20), the spectral integration is performed strictly along the real-k_y axis and the residue contributions at $\pm k_{yp}$ (see Fig. 8) are simply ignored. However, as it can be analytically shown, (20) is not equivalent to the correct procedure in (17)–(19), where the growing fields have been properly extracted out by explicit removal of the spectral singularities at $\pm k_{yp}$.

Using the bound mode power, P_b, we define a new "bound mode characteristic impedance," Z_c, for a slot-type line as

$$Z_c = \frac{|V_0|^2}{P_b^*}. \quad (21)$$

Similarly, for a strip-type line the new characteristic impedance can be defined using the total strip current, I_0, and the bound mode power, P_b, as

$$Z_c = \frac{P_b^*}{|I_0|^2}. \quad (22)$$

The Z_c as defined above is the "equivalent characteristic impedance," that should realistically model the impedance characteristics of a practical finite-length section of the leaky transmission line. When the transmission line is dominantly leaky, this definition of characteristic impedance should be used for circuit modeling. Like a standard lossy transmission line with purely material loss [16], here the bound mode characteristic impedance, Z_c, for a transmission line with leakage loss will also be a complex number with real and imaginary parts.

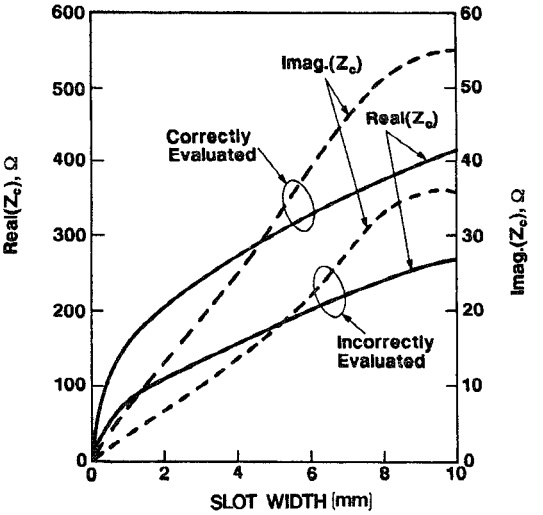

Fig. 9. Real and imaginary parts of the characteristic impedance, Z_c, computed using the bound mode power, P_b, in (19), for an infinite-length conductor-backed slotline geometry. The uniform dielectric constant between the parallel plates = 2.55, with thickness = 0.8 cm. No cover substrate on top, frequency = 10 GHz. The corresponding results of Z_c, using the incorrectly evaluated bound mode power, P_b', in (20), are also shown for comparison. P_b' is incorrectly evaluated along the real k_y axis, without properly extracting the growing fields.

A. Results

Fig. 9 shows the real and imaginary parts of the characteristic impedance, Z_c, of a conductor-backed slotline computed using the bound-mode power P_b in (19), for different values of the slot widths. As expected, the magnitude of the characteristic impedance has an increasing trend as the slot width increases, starting with a zero value when the slot width is zero. The corresponding values of the real and imaginary parts of the Z_c, if the propagating power, P_b, is incorrectly computed as P_b' in (20), are also shown for reference. Clearly, significant differences would result if the power is not properly evaluated with correct extraction of the bound field components, as discussed in the last section.

For the same parameters of Fig. 9, the values of the equivalent characteristic impedances, Z_c, were separately calculated from the input impedance seen by a delta-gap source connected at the center of a finite-length stub section. The 3-D moment method analysis of Section II was used for the computation. This procedure is fundamentally independent of the computation of Z_c in Fig. 9. For the finite-length section of Fig. 1, the input impedance, Z_{in}, seen by the delta-gap current source can be expressed as

$$Z_{in} = \frac{V(x=0)}{I} = V(x=0) = V_0 \quad (23)$$

where V_0 is the slot voltage at the location of the delta-gap source. V_0 is computed from the moment method solution, and is equal to the coefficient of the zeroth basis function in (2). Using a circuit equivalent of the two short-circuited slotline stubs in Fig. 1, seen in parallel with each other across the delta-gap at the center, the equivalent characteristic impedance can now be derived from the above input impedance, Z_{in}

$$Z_c = \frac{2Z_{in}}{j\tan[(\beta - j\alpha)L]} = \frac{2V_0}{j\tan[(\beta - j\alpha)L]}. \quad (24)$$

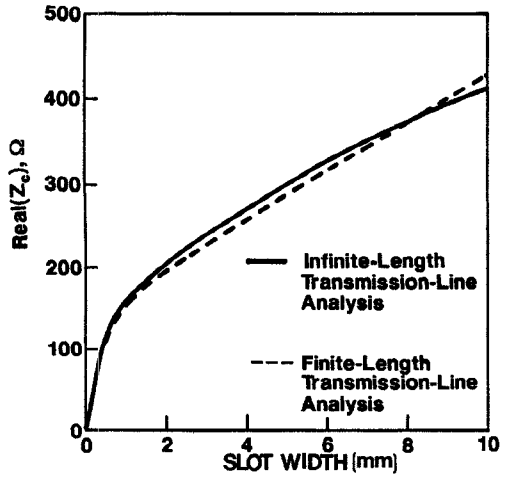

Fig. 10. Comparison of the "equivalent characteristic impedances" seen by a delta-gap current source across the center of a finite-length conductor-backed slotline section, and the corresponding values from Fig. 9 obtained using the new definition of the characteristic impedance.

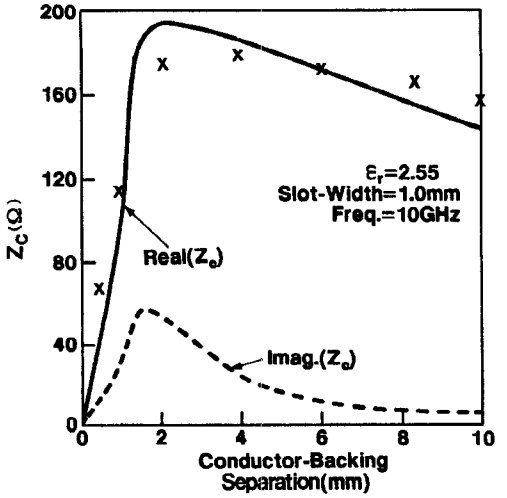

Fig. 11. Computed values of the characteristic impedance for an ideal infinite-length conductor-backed slotline, obtained using the bound-mode power, P_b, as a function of the thickness of the substrate ($\epsilon_r = 2.55$) between the parallel plates. The real parts are compared with that derived from the input impedance of a finite-section (x x x x). Slot width = 0.1 cm, frequency = 10 GHz.

The phase constant, β, and attenuation constant, α, in (24) can be obtained from Fig. 3, either using an ideal infinite-length analysis, or from a moment method analysis of the finite-length section. When the two parallel stubs in Fig. 1 are not of equal length, (24) can be substituted by a different circuit equation accommodating for the unequal stub lengths. Note that the moment method computation of Z_{in} in (23) rigorously include the discontinuity effects at the stub ends, as well as the mutual coupling between the two stubs, whereas the circuit equivalent modeling of (24) does not include these effects. These are the potential sources of error in the use of (24), but are usually negligible causing second-order corrections.

The real parts of characteristic impedances computed using (24) are compared in Fig. 10 with the results of Fig. 9. Similar results for the conductor-backed slotline for different values of thickness, D, of the parallel-plate substrate, independently obtained from a rigorous finite-length analysis [using (24)] and our new characteristic impedance definition [using (19), (21)], are compared in Fig. 11. Several computations were done with different stub lengths, and with the same or different lengths of the two stubs in the two sides of the excitation source, giving consistent results. As the comparisons in Figs. 10 and 11 confirm, the characteristic impedance obtained from the analysis of an infinite-length leaky line, using the new definition in (19) and (21), does accurately model the impedance behavior of practical finite-length stub sections. In Figs. 10 and 11 only the real parts of the characteristic impedances are compared with independent computations. As seen from the results of Figs. 9 and 11, the corresponding imaginary parts have significantly lower magnitudes compared to the real parts, and hence could not be accurately extracted from the input impedance, Z_{in}, seen by the delta-gap source. The additional reactive impedance, due to the additional reactive fields in the vicinity of the delta-gap discontinuity (see Fig. 1), is likely to have masked the smaller reactive contribution due to the complex characteristic impedance of the slotline.

Characteristic admittance results similar to Fig. 10, but for a two-layer stripline, are presented in Fig. 12. The results in Fig. 12 are for the characteristic admittances, $Y_c = G_c + jB_c$, in contrast to the characteristic impedance results for the dual situation of a leaky slotline. The real parts, G_c, in Fig. 12, derived from the input admittance of the finite stub geometry, are also seen to compare well with that of the bound-mode characteristic impedance of (19) and (22). This result further validates our new definition of the characteristic impedance for strip-type leaky lines, as well.

IV. Leakage-Transition Behavior on Practical Finite-Length Transmission Lines

The intersecting region between a guided-mode of a printed transmission line, and the characteristic background mode of the substrate structure to which the leakage power couples to, is referred to as the "mode-transition" region. In one side of the transition, where the propagation constant of the transmission line mode is greater than that of the characteristic substrate-mode, the transmission line mode is nonleaky. This nonleaky mode changes over to a leaky mode as it crosses to the other side of the transition. The above interpretation only provides a simplistic picture. If designed around the crossover region, the transmission line and the substrate-mode fields strongly interact with each other, resulting in a complex multimodal behavior.

As examples, we have shown such transition behavior in Figs. 13 and 15 for a conductor-backed covered slotline and a two-layer stripline, respectively, assuming an ideal infinite-length extension. The splitting of the two modes in Figs. 13 and 15 due to the mutual interaction between them is clearly seen. Similar multimodal behavior in ideal infinite-length lines have also been demonstrated for other printed lines [5], [17], as well as for other guided waves [18]. For a practical finite-length section of a leaky line, however, the actual excitation in this transition region is much more complex, involving combinations of the multiple leaky and nonleaky modes. In

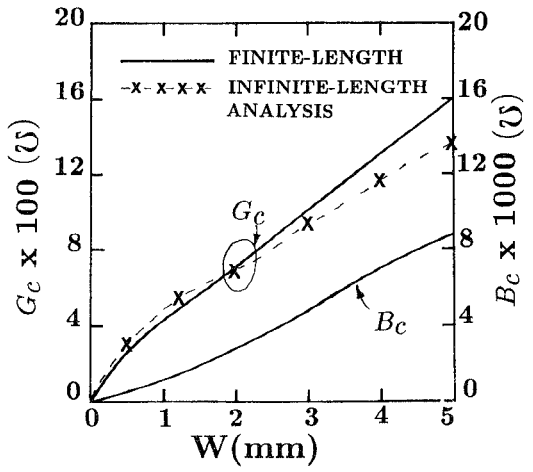

Fig. 12 The real parts of the equivalent characteristic admittance, $Y_c = G_c + jB_c$, of the two-layer stripline of Fig. 15, derived from the input impedance of a finite-length stub section, as compared with the corresponding values obtained using the new "bound-mode characteristic impedance" definition. The input impedance from which the above characteristic impedances were derived is computed as seen across a delta-gap voltage source at the center of the finite-length stub section (see Fig. 16 for the stub geometry and excitation), $h = 10$ mils, and W is the width of the stripline. The poorer comparison of results for larger W is due to the gradual excitation of the additional nonleaky mode of the stripline (see Fig. 15), which the new definition of characteristic impedance does not account for.

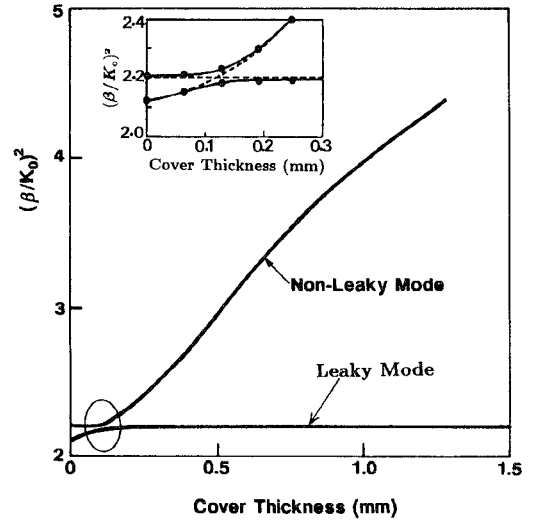

Fig. 13. Phase constant, β, of a conductor-backed slotline with a dielectric cover on top, as a function of the cover thickness. Slot width = 0.1 cm; conductor-backing substrate: $\epsilon_r = 2.2$, thickness = 0.16 cm; frequency = 10 GHz; dielectric constant of the cover substrate = 10.2. Two possible modes are seen with a mode-transition around the region where both modes have approximately the same propagation constants. The magnified details of the mode transition region are also shown as the inset Notice that parts of the two modes are similar to a parallel-plate mode, with $(\beta/k_0)^2 \simeq 2.2$.

order to understand the interesting mode transition behavior in a practical circuit, it is important to perform a rigorous 3-D analysis of a finite-length section of the transmission line with a specific source structure.

For the conductor-backed covered slotline section of Fig. 13, we have used the 3-D analysis of section 2.0. Six different values of the cover thickness are selected around as well as away from the transition region. The results of

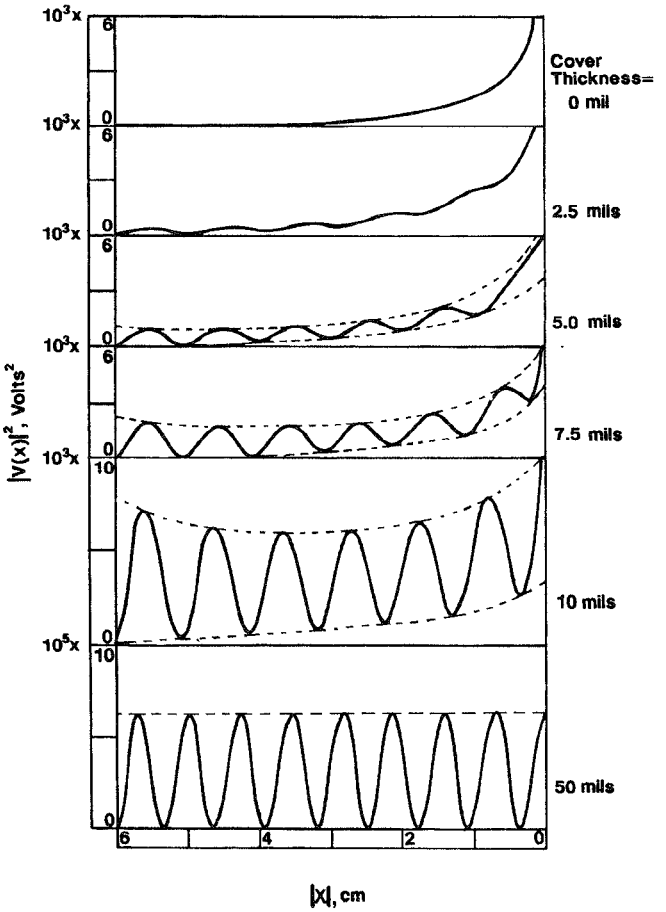

Fig. 14. Voltage along a finite-length section of the conductor-backed slotline geometry of Fig. 13, for different values of the cover thicknesses. $2L = 12$ cm (see Fig. 1), and the delta-gap current source = 1.0 A. The different values of the cover thicknesses are particularly chosen around the mode-transition region of Fig. 13, and correspond to the identified points on the magnified inset diagram of Fig. 13.

variation of the slot-voltages are plotted in Fig. 14 as a function of the position along the slot-section. As in Fig. 2, the attenuation level can be estimated from the variations of voltage in Fig. 14. The relative level of the lower envelope of the $|V(x)|^2$ variation, compared to the amplitude of oscillation, is the measure of the attenuation constant, α. It should also be noted, due to the anticipated multimodal excitation, in Fig. 14 we should expect a combination of an attenuating and a nonattenuating modes with different propagation constants.

In Fig. 14, for the two extreme cases without any cover substrate and with a thick cover substrate (the top and bottom curves, respectively), clearly the excited modes are dominantly leaky and nonleaky, respectively. The values of α and β for these extreme cases, calculated from the $|V(x)|^2$ variations as done in Fig. 2, also compare well with the corresponding values from an ideal infinite-length analysis. Interestingly, for intermediate values of the cover thicknesses close to the transition region (correspond to four graphs in the middle of Fig. 14), the excitation characteristics can be seen to gradually transform from a dominantly leaky to a dominantly nonleaky mode, as the cover thickness increases.

Notice in Fig. 14 that for a cover thickness of 0.254 mm (10 mils), which is above the threshold value at transition

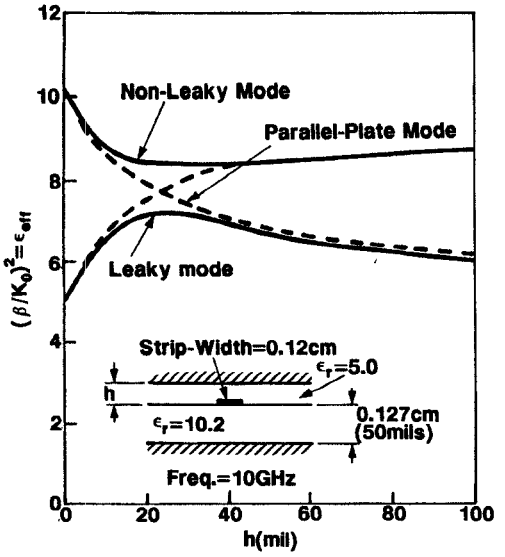

Fig. 15. Phase constant, β, of a two-layer stripline as a function of the thickness, h, of the top substrate. Strip-width = 0.12 cm; top-substrate dielectric constant = 5.0; bottom substrate: dielectric constant = 10.2, thickness = 0.127 cm (50 mils); frequency = 10 GHz. Two possible modes are seen, with a mode transition behavior similar to that in Fig. 13.

(≃0.12 mm), the excited mode is still significantly leaky. This suggests that the leakage level can be significant, even when the operating point is above the transition threshold. The slow modulation of the amplitude of oscillation can be clearly seen for thickness = 10 mils, as well as for the cover thicknesses of 5.0 mils and 7.0 mils but to a smaller level. This is due to the superposition of two excited modes (one leaky and the other nonleaky) with comparable amplitudes and slightly different propagation constants. The above results caution that in order to avoid leakage one must operate sufficiently above a mode-transition zone. In other words, the no-leakage condition as stated in [2], [15], and [1] that requires to have the propagation constant of a transmission line greater than all surface characteristic modes of the substrate layering, is not a sufficient condition for practical finite-length sections. In order to precisely determine a safe zone of operation for practical circuits, results similar to Fig. 14 may be used to ensure that the nonleaky mode is the dominant form of excitation.

Leakage-transition results quite similar to Fig. 14, but for a strip-type transmission line of Fig. 15, are shown in Fig. 16. When the top substrate thickness, h, is sufficiently large, the two-layer stripline in Fig. 16 is seen to be purely nonleaky. The leakage attenuation is significant for values of h around the transition region, but can be seen to be still significant (see for h = 50 mils) even when h is larger than the transition value (≃25 mils). For example, when h = 100 mils, which is quite larger than the transition value, appreciable power leakage can be seen in Fig. 16. On the other hand, when the value of h is much smaller (10 mils or smaller) than the transition value, the leaky mode is excited to a dominant level. This is confirmed by comparing the propagation constant derived from Fig. 16 with that of the leaky mode of Fig. 15. However, the attenuation constant, α, of the leaky stripline mode is small when the top-substrate is significantly thinner than the bottom substrate. Accordingly, the attenuation behavior in Fig. 16 is seen to

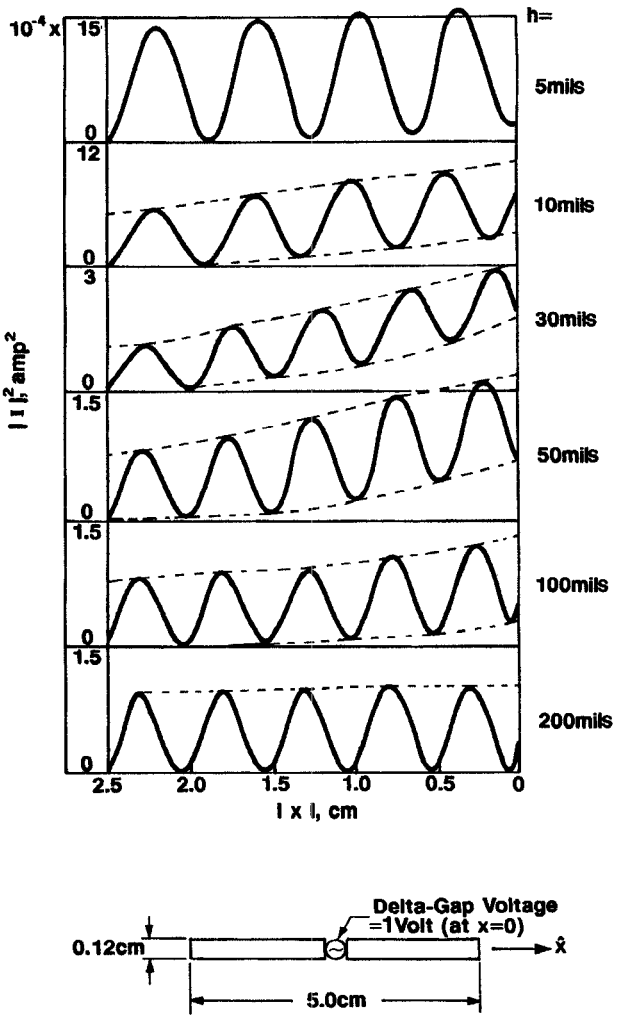

Fig. 16. Current along a finite-length section of the two-layer stripline of Fig. 15, for different values of the top-substrate thickness, h. The length of the finite-length section = $2L$ = 5.0 cm. The delta-gap voltage source is at the center (x = 0). The different values of h are chosen around the mode transition region of Fig. 15.

have decreased when h is reduced below the transition value of about 25 mils. If the top-substrate thickness is 5 mils or less, even though the leaky mode is the dominant mode of excitation, the transmission line can be practically treated as a nonleaky line due to its significantly low level of attenuation.

V. Conclusion

Our investigation casts several new insights into the characteristics of leakage in practical situations of finite-length circuits. The demonstrative results and conclusions for the finite-length stub geometries we have presented should be applicable to other general finite-length circuits as well. The possibilities of power leakage in a printed transmission line, due to the radiation as well as excitation of the surface-guided modes, are analytically confirmed for the finite-stub geometries. The new definition of the characteristic impedance for a leaky line, based on the "bound mode power," is shown to correctly model the impedance characteristics of the finite-length stub sections. When the propagation along the printed transmission line is known to be dominantly leaky, this

new definition should be used for practical circuits, instead of the standard definitions of the characteristic impedance commonly used for nonleaky lines. In addition, the interesting gradual transition behavior of leakage across the "mode-transition" region is demonstrated for the finite-length stub sections of strip- and slot-type transmission lines. This clearly demonstrates that in order to avoid any leakage problems in a practical circuit, one should design sufficiently above, not just above, the mode-transition point. Such new results of practical significance should find valuable applications in integrated circuit designs, allowing reliable avoidance or novel use of the leakage behavior.

REFERENCES

[1] H. Shigesawa, M. Tsuji, and A. A. Oliner, "Conductor backed slotline and coplanar waveguide: Dangers and fullwave analyses," in *IEEE Microwave Theory Tech. Symp. Dig.,* 1988, pp. 199–202.

[2] N. K. Das and D. M. Pozar, "Full-wave spectral-domain computation of material, radiation, and guided wave losses in infinite multilayered printed transmission lines," *IEEE Trans. Microwave Theory Tech.,* vol. 39, no. 1, pp. 54–63, Jan. 1991.

[3] D. S. Phatak, N. K. Das, and A. P. Defonzo, "Dispersion characteristics of optically excited coplanar striplines: Comprehensive full-wave analysis," *IEEE Trans. Microwave Theory Tech.,* vol. 38, no. 11, pp. 1719–1731, Nov. 1990.

[4] L. Carin and N. K. Das, "Leaky waves in broadside-coupled microstrips," *IEEE Trans. Microwave Theory Tech.,* vol. 40, no. 1, pp. 58–66, Jan. 1992.

[5] M. Tsuji, H. Shigesawa, and A. Oliner, "New interesting leakage behavior on coplanar waveguides of finite and infinite widths," *IEEE Trans. Microwave Theory Tech.,* vol. 39, no. 12, pp. 2130–2137, Dec. 1991.

[6] N. K. Das and D. M. Pozar, "Multiport scattering analysis of multilayered printed antennas fed by multiple feed ports, part I: Theory; Part II: Applications," *IEEE Trans. Antennas Propagat.,* vol. 40, no. 5, pp. 469–491, May 1992.

[7] W. E. McKinzie and N. G. Alexopoulos, "Leakage losses for the dominant mode of conductor-backed coplanar waveguide," *IEEE Microwave Guided Wave Lett.,* vol. 2, no. 2, pp. 65–66, Feb. 1992.

[8] E. H. Newman, "An overview of the hybrid MM/Green's function method in electromagnetics," *Proc. IEEE,* vol. 76, no. 3, pp. 270–282, Mar. 1988.

[9] D. M. Pozar, "Input impedance and mutual coupling of rectangular microstrip antennas," *IEEE Trans. Antennas Propagat.,* vol. AP-30, no. 6, pp. 1991–1996, Nov. 1982.

[10] J. R. Mosig, "General integral equation formulation of microstrip antennas and scatterers," *Proc. IEE,* Pt-H, vol. 132, no. 7, pp. 424–432, 1985.

[11] P. B. Katehi and N. G. Alexopoulos, "On the modeling of electromagnetically coupled microstrip antennas—The printed strip dipole," *IEEE Trans. Antennas Propagat.,* vol. AP-32, no. 11, pp. 1179–1186, Nov. 1984.

[12] N. K. Das and D. M. Pozar, "A generalized CAD model for printed antennas and arrays with arbitrary multilayer geometries," in *Computer Physics Communication, Thematic Issue on Computational Electromagnetics.* L. Safai, Ed. New York: North-Holland, 1991.

[13] ——, "A generalized spectral-domain Green's function for multilayer dielectric substrates with applications to multilayer transmission lines," *IEEE Trans. Microwave Theory Tech.,* vol. MTT-35, no. 3, pp. 326–335, Mar. 1987.

[14] N. K. Das, "A study of multilayered printed antenna structures," Ph.D. dissertation, Dept. Electrical and Computer Eng., Univ. Massachusetts, Amherst, Sept. 1987.

[15] ——, "Spectral-domain modeling of radiation and guided wave leakage in printed transmission lines," in *Proc. Int. Conf. on Directions in Electromagnetic Wave Modeling,* Polytechnic Univ., NY, H. L. Bertoni and L. B. Felsen, Eds. New York: Plenum, Oct. 1990, pp. 363–370.

[16] D. M. Pozar, *Microwave Engineering.* Reading, MA: Addison-Wesley, 1990.

[17] M. Tsuji, H. Shigesawa, and A. Oliner, "New surface-wave-like mode on CPW's of infinite widths and its role in explaining the leakage cancellation effect," in *IEEE Microwave Theory Tech. Soc. Symp. Dig.,* 1992, pp. 495–498.

[18] H. A. Haus, *Waves and Fields in Optoelectronics.* Englewood Cliffs, NJ: Prentice-Hall, 1984.

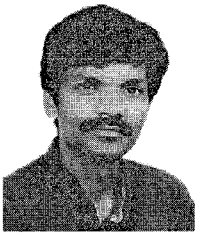

Nirod K. Das (S'89–M'89) was born in Puri, Orissa State, India, on February 27, 1963. He received the B.Tech (Hons.) degree in electronics and electrical communication engineering from the Indian Institute of Technology (IIT), Kharagpur, India, in 1985, and the M.S. and Ph.D. degrees in electrical engineering from the University of Massachusetts, Amherst, in 1987 and 1989, respectively.

From 1985 to 1989 he was with the Department of Electrical and Computer Engineering at the University of Massachusetts, Amherst, first as a Graduate Research Assistant and then, after receiving the Ph.D. degree, as a Postdoctoral Research Associate. In 1990, he joined the Department of Electrical Engineering at Polytechnic University, Farmingdale, NY, as an Assistant Professor. His research interests have been in the general areas of microwave, millimeter wave, and optoelectronic integrated circuits and antennas. In particular, his recent research has been focused on the analytical and experimental study of multiple layered structures for integrated circuit and phased array applications.

Dr. Das has received a student prize paper award from the U.S. National Council of URSI, and the 1992 R.W.P. King Best Paper Award from the Antennas and Propagation Society of IEEE, for his multilayer printed antenna work.